JOC The Journal of Organic Chemistry

pubs.acs.org/joc Article

Melicopteline A–E, Unusual Cyclopeptide Alkaloids with Antiviral Activity against Influenza A Virus from *Melicope pteleifolia*

Ba Wool Lee, Thi Kim Quy Ha, Eun Jin Park, Hyo Moon Cho, Byeol Ryu, Thi Phuong Doan, Hee Ju Lee, and Won Keun Oh*

Cite This: *J. Org. Chem.* 2021, 86, 1437–1447 Read Online

ACCESS | Metrics & More | Article Recommendations | Supporting Information

ABSTRACT: In the search for antiviral cyclopeptides against influenza A virus, five unprecedented Caryophyllaceae-type cyclopeptides (**1**–**5**) were isolated from the leaves of *Melicope pteleifolia*. Their chemical structures and absolute configurations were unambiguously determined by means of advanced Marfey's analysis and comprehensive spectroscopic analyses including two-dimensional nuclear magnetic resonance and MS/MS fragmentation. Interestingly, compounds **3**–**5** contain an unusual heterocycle, a 3a-hydroxypyrroloindole moiety, which was biosynthetically formed by a nucleophilic cyclization from the least abundant amino acid, tryptophan, precursor and has aroused a great interest in the aspect of chemical diversity and biological activity. All isolates (**1**–**5**) were evaluated for their protective effects against influenza A viruses H1N1 and H9N2 in MDCK cells. All isolated cyclopeptides exhibited strong anti-influenza activity, especially against H1N1. Compound **3** showed the most potent CPE inhibition effect, which was stronger than that of the positive control ribavirin against H1N1, with an EC_{50} (μM) of 2.57 ± 0.45 along with higher selectivity.

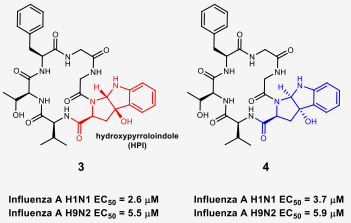

INTRODUCTION

The hexahydropyrrolo[2,3-*b*]indole (HPI) skeleton has attracted great attention in the field of natural product chemistry, synthetics, and biology in the aspect of structural diversity and its myriad range of biological activities.[1] Various types of compounds containing HPI have been reported from marine organisms, plant sources, and amphibians such as frogs. Structurally, they vary from simple alkaloids containing HPI, for example, (+)-alline,[2] (−)-physostigmine,[3] or the flustramine[4] family, to more complex ones, such as ardeemins[5] and amauromine[6] with two units of HPI and also echitamine[7] with fused ring systems. Although there are some HPI-containing compounds, only a few cyclopeptides comprising the HPI motif from natural products (extremely rare from higher plants) have been reported to date. There are representative cases with their biological properties such as nematicidal activity of omphalotin D,[8] antineoplastic property of phakellistatin 3,[9] spore germination-inhibiting activity of kutzneride 1′ against several root-rotting fungi,[10] antitumor and antibiotic properties of himastatin,[11] and chloptosin as an apoptosis-inducing agent.[12] All of the aforementioned cyclopeptides contain 3a-hydroxylated HPI, which is called "photo-Trp", as it is derived from a photooxidation product of tryptophan.[13]

Traditionally, *Melicope pteleifolia* has long been used for the treatment of various diseases or symptoms, including cerebritis, eczema, dermatitis, rheumatoid arthritis, cold, and flu accompanying high fever and pain, as tea or traditional Chinese medicine granules in China and Vietnam.[14−16] Especially, *M. pteleifolia* has been currently utilized as a main raw material in various preparations such as Sanjiu weitai granules, Sanjin cold tablets, and Zhiganjia capsules to treat gastritis, rhinitis, influenza, and other diseases in China.[17−19] From modern pharmacological investigation, it has been reported that extracts or compounds obtained from *M. pteleifolia* showed anti-inflammatory,[20] antinociceptive,[21] anticancer,[22] and anti-influenza A virus activity.[15] Moreover, our previous studies on *M. pteleifolia* have demonstrated that the phloroacetophenone derivatives dominantly present in the plant play an important role in recovery from cold by lowering excessive heat in the animal model, by which we proved scientifically ethnopharmacological uses of the plant.[23]

Through the acid−base extraction method, alkaloid-enriched fractions enabled us to isolate efficiently five Caryophyllaceae-type cyclopeptides (**1**–**5**). Especially, compounds **3**–**5** possess a rare HPI moiety in their structures (Figure 1). Considering the observation and that many cyclopeptides have been reported to show inhibitory activity against various microbes including viruses, the isolates (**1**–**5**) were evaluated for their

Received: September 4, 2020
Published: December 28, 2020

https://dx.doi.org/10.1021/acs.joc.0c02137
J. Org. Chem. 2021, 86, 1437−1447

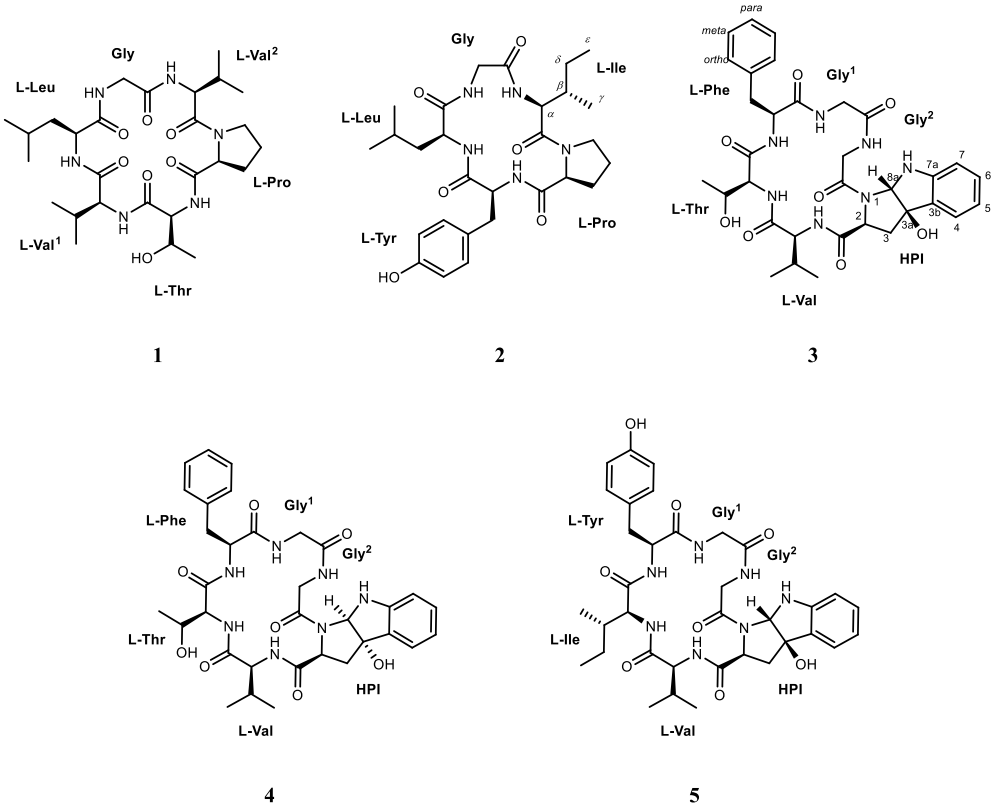

Figure 1. Structures of cyclopeptides isolated from *M. pteleifolia*. Compounds **3**–**5** contain the unusual motif hydroxypyrroloindole (HPI).

protective effects against influenza A virus H1N1 and H9N2 subtypes by performing a cytopathic effect inhibition assay.

RESULTS AND DISCUSSION

Melicopteline A (**1**) was obtained as a yellow and amorphous solid. Its molecular formula was established as $C_{27}H_{46}N_6O_7$ based on its protonated high-resolution electrospray ionization mass spectrometry (HRESIMS) ion peak at m/z 567.3517 $[M + H]^+$ (calcd for $C_{27}H_{47}N_6O_7$, 567.3506) corresponding to eight degrees of unsaturation. The IR spectrum demonstrated the presence of amine (3311 cm^{-1}) and amide (1638 cm^{-1}) groups. The characteristics of the peptide, which are five exchangeable amide NH signals (δ_H 7.5–8.5), seven amino acid α-proton signals (δ_H 3.5–5.0), and 19 aliphatic methane, methylene, and methyl signals (δ_H 0.0–4.5), were observed in the ^1H nuclear magnetic resonance (NMR) spectrum of **1** (Table 1). Moreover, the $^{13}C\{^1H\}$ NMR spectrum showed six distinguishable signals for amide-type carbonyl groups (δ_C 169.4–172.1). All of the protons and the corresponding carbons were precisely matched by analyzing the HSQC spectrum, and the subsequent bonding of protons within the same spin systems of each amino acid was correlated through COSY spectrum analysis, thus identifying every constituent amino acid residues to be two valines (Val), threonine (Thr), leucine (Leu), glycine (Gly), and proline (Pro). ROESY and HMBC spectra of **1** (Figure 2) were analyzed to assemble these units of amino acid, but the full sequence could not be accomplished by HMBC and ROESY correlations because of highly similar signals (δ_C 169.42, 169.48, 171.02, and 171.03) and some missing correlations from nitrogen protons to the adjacent carbons. HMBC correlations from the NH-proton (δ_H 8.40, d, J = 4.8 Hz) of Val^1 and the α-proton (δ_H 4.52, dd, J = 9.8, 5.4 Hz) of Thr to the carbonyl carbon (δ_C 172.1) of Thr demonstrated the connectivity of Val^1 and Thr.

The ROESY correlations between the NH-proton (δ_H 7.12, t-like) of Gly and the α-proton (δ_H 4.06, t, J = 8.4 Hz) of Leu, between the α-proton (δ_H 3.73, overlap) of Gly and the NH-proton (δ_H 7.93, br s) of Val^2, and between the α-proton (δ_H 4.23, overlap) of Val^2 and the α-proton (δ_H 4.45, br d, J = 8.0 Hz) of Pro suggested the linkage of the Leu–Gly–Val^2–Pro sequence.

In order to link the partial sequences (Thr–Val^1 and Leu–Gly–Val^2–Pro), MS/MS fragmentation patterns in the positive mode were analyzed. Considering that cleavage occurs predominantly at the N-terminal for Pro when Val, His, Asp, Ile, and Leu are located right before Pro, based on the "proline effect", the protonated ion at m/z 567 $[M + H]^+$, subsequent MS/MS fragments at m/z 468, 298, and 199, and their corresponding dehydrated ions at m/z 450, 280, and 181 were detected. The sequential losses of Val^2, Gly, Leu, Val^1, and H_2O from the remaining Thr were also observed, indicating a cleavage between Val^2 and Pro (Figure S9 and Table S1).[24] The partial sequences due to the sequential losses and the above-mentioned results indicated that compound **1** is linked in a cyclo-sequence (Pro–Thr–Val^1–Leu–Gly–Val^2) (Figure 3).

For the determination of the absolute configuration of each amino acid α-carbon, the advanced Marfey's method was implemented (Table S2 and Figure S44). Compound **1** was hydrolyzed and derivatized with L-FDLA (N^{α}-(5-fluoro-2,4-dinitrophenyl)-L-leucinamide). Retention times and mass by liquid chromatography/mass spectrometry analysis were compared with those of the derivatives of standard amino acids.[25] The results showed the absolute configuration for Pro, Val, Thr, and Leu residues to be L configurations. Especially, as

https://dx.doi.org/10.1021/acs.joc.0c02137
J. Org. Chem. 2021, 86, 1437–1447

Table 1. ^{1}H NMR Data [δ_H in ppm, Multiplicity (J in Hz)] for Compounds 1−5[a]

position	1		2		3		4		5	
Pro		Pro		HPI		HPI		HPI		
α	4.45, br d (8.0)	α	4.37, d (8.6)	2	4.16, overlap	2	4.76, dd (10.4, 6.0)	2	4.18, overlap	
β	2.18, dd (12.1, 6.4); 1.93, m	β	1.99, m; 1.70, m	3	2.40, dd (12.8, 9.6); 2.29, dd (13.6, 4.8)	3	2.76, dd (14.2, 10.4); 2.05, dd (14.2, 5.9)	3	2.41, m; 2.32, dd (16.7, 4.4)	
γ	1.84, m; 1.67, overlap	γ	1.71, m; 1.45, m	4	7.25, d (7.5)	4	7.21, d (7.5)	4	7.26, d (7.2)	
δ	3.52, ddd (11.5, 11.5, 7.2); 3.40, m	δ	3.46, m; 3.40, m	5	6.75, t (7.4)	5	6.79, t (7.4)	5	6.75, t (8.0)	
Thr		Tyr		6	7.11, t (7.6)	6	7.11, t (7.9)	6	7.12, ddd (8.0, 8.0, 1.6)	
α	4.52, dd (9.8, 5.4)	α	4.48, dd (14.8, 7.9)	7	6.66, d (7.9)	7	6.60, d (7.9)	7	6.66, d (8.0)	
β	4.24, overlap	β	2.80, m	8a	5.63, d (3.9)	8a	5.58, d (4.7)	8a	5.65, d (4.8)	
γ	1.04, d (6.3)	*ortho*	6.91, d (8.1)	NH	6.90, d (4.5)	NH	7.20, overlap	NH	6.90, d (4.5)	
NH	8.20, br s	*meta*	6.62, d (8.5)	OH	6.17, br s	OH		OH	6.29, br s	
OH	5.15, br s	NH	7.09, d (7.2)	Val		Val		Val		
Val[1]		Leu		α	4.14, overlap	α	4.11, dd (10.5, 4.4)	α	4.16, overlap	
α	3.74, dd (11.3, 5.3)	α	3.86, m	β	2.11, m	β	2.10, m	β	2.11, m	
β	2.09, m	β	1.55, m	γ	0.86, d (6.8)	γ	0.50, d (6.9)	γ	0.86, d (6.4)	
γ	0.95, d (6.7)	γ	1.43, m		0.87, d (6.8)		0.35, d (6.9)		0.88, d (7.2)	
	0.94, d (6.9)	δ	0.87, d (6.6); 0.81, d (6.7)	NH	7.92, d (12.0)	NH	7.53, d (10.0)	NH	7.79, d (9.9)	
NH	8.40, d (4.8)	NH	8.66, d (7.4)	Thr		Thr		Ile		
Leu		Gly		α	4.30, dd (6.7, 2.9)	α	4.13, dd (5.3, 3.8)	α	4.28, m	
α	4.06, t (8.4)	α	4.15, dd (15.0, 8.6); 3.16, dd (14.7, 2.4)	β	4.02, br s	β	4.05, m	β	1.68, m	
β	1.67, overlap; 1.55, overlap	NH	7.19, br d (7.6)	γ	0.95, d (6.2)	γ	1.00, d (6.5)	γ	0.77, d (7.2)	
γ	1.51, overlap	Ile		NH	7.55, d (6.9)	NH	7.11, d (7.0)	δ	0.89, m	
δ	0.86, d (6.6); 0.82, d (6.4)	α	4.35, t (9.0)	OH	5.19, br s	OH		ε	0.74, t (7.2)	
NH	8.14, br s	β	1.80, m	Phe		Phe		NH	7.45, d (1.6)	
Gly		γ	0.73, d (6.8)	α	4.15, overlap	α	4.27, m	Tyr		
α	3.73,overlap; 3.49, dd (15.7, 4.1)	δ	0.99, overlap	β	3.18, dd (14.2, 5.5); 2.89, dd (14.2, 9.3)	β	2.99, dd (13.9, 6.4); 2.89, dd (13.9, 8.8)	α	4.05, m	
NH	7.12, t-like	ε	0.79, t (7.5)	*ortho*	7.27, m	*ortho*	7.24, m	β	3.05, dd (14.3, 5.8); 2.79, dd (14.4, 9.1)	
Val[2]		NH	7.95, d (9.0)	*meta*	7.29, m	*meta*	7.31, t (7.6)	*ortho*	6.99, d (8.0)	
α	4.23, overlap			*para*	7.21, t (6.9)	*para*	7.24, t (6.7)	*meta*	6.66, d (8.0)	
β	2.02, m			NH	8.22, d (4.4)	NH	7.95, d (4.3)	NH	8.23, s	
γ	0.87, d (6.9); 0.96, d (6.9)			Gly[1]		Gly[1]		Gly[1]		
NH	7.93, br s			α	3.94, dd (16.8, 7.3); 3.41, dd (16.9, 4.8)	α	3.87, dd (17.0, 7.1); 3.43, dd (17.0, 5.0)	α	3.95, dd (16.7, 7.5); 3.36, dd (16.8, 4.4)	
				NH	8.66, t (5.5)	NH	8.86, t (5.9)	NH	8.46, br s	
				Gly[2]		Gly[2]		Gly[2]		
				α	4.50, dd (17.0, 8.2); 3.89, d (16.8)	α	4.51, dd (17.8, 8.1); 3.98, d (17.4)	α	4.47, m; 3.81, d (15.6)	
				NH	7.90, overlap	NH	8.04, d (8.0)	NH	8.14, br d (7.2)	

[a]Data were measured in DMSO-d_6 at 800 MHz.

isomers of Thr show peaks of very similar retention times because of their one more stereogenic center at the β position, their configuration was determined unambiguously to be L-Thr using different high-performance liquid chromatography (HPLC) conditions equipped with MS (Figure S45). A strong ROESY correlation between the α-proton (δ_H 4.45, br d, J = 8.0 Hz) of Pro and the α-proton (δ_H 4.23, overlap) of Val[2] and the $\Delta\delta_{C\beta-C\gamma}$ values (9.4 ppm) of Pro suggested that the amide bond of Val[2]-Pro was in a *cis* configuration (Figure 2 and Table 2).[26,27] Consequently, the structure of **1** was fully determined to be cyclo (L-Pro−L-Thr−L-Val[1]−L-Leu−Gly−L-Val[2]).

Melicopteline B (**2**) was isolated as a pale yellow and amorphous solid. The molecular formula of **2** was established as $C_{28}H_{41}N_5O_6$ based on a HRESIMS ion peak at m/z 544.3134 $[M + H]^+$, corresponding to 11 degrees of unsaturation index. The comparison of ^{1}H and $^{13}C\{^1H\}$ NMR spectra (Tables 1 and 2) of **2** with those of **1** indicated that **2** has Pro, Leu, and Gly, which were also confirmed by HMBC and COSY NMR analyses. The double intensity peaks at δ_C 130.0 and 114.8 and the double integration of the proton peaks with doublet splitting patterns at δ_H 6.91 and 6.62 were characteristics of tyrosine (Tyr), which was also verified by two-dimensional (2D) NMR analysis. The combined HSQC,

https://dx.doi.org/10.1021/acs.joc.0c02137
J. Org. Chem. 2021, 86, 1437−1447

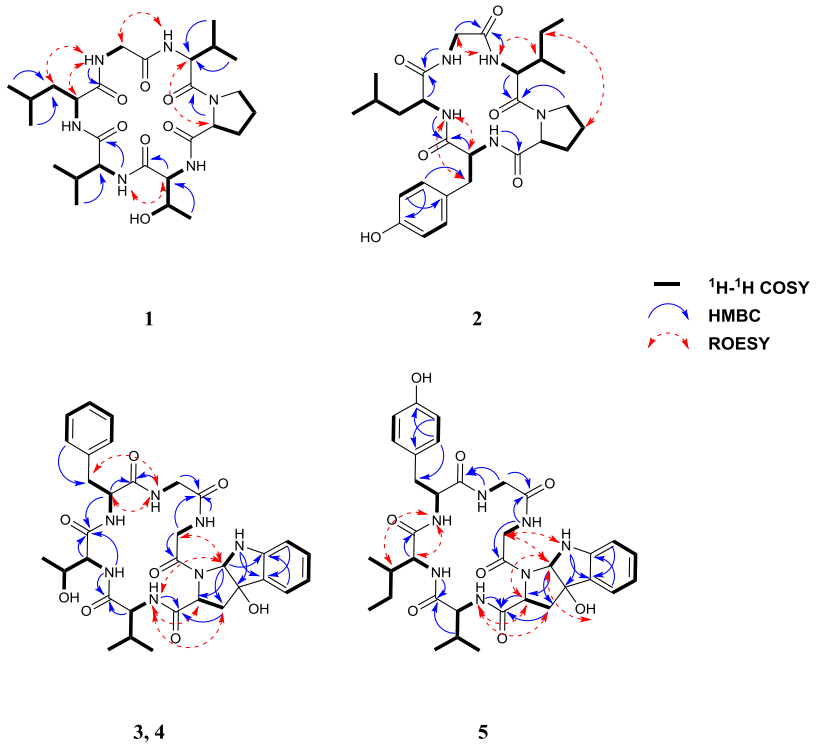

Figure 2. (A) Key correlations of COSY (bold), HMBC (arrows), and ROESY (dashed arrows) of compounds **1**−**5**. The key ROESY correlations were present for the confirmation of the linkage of structures because of the highly overlapped carbon signals and a few faint correlations in the HMBC spectrum.

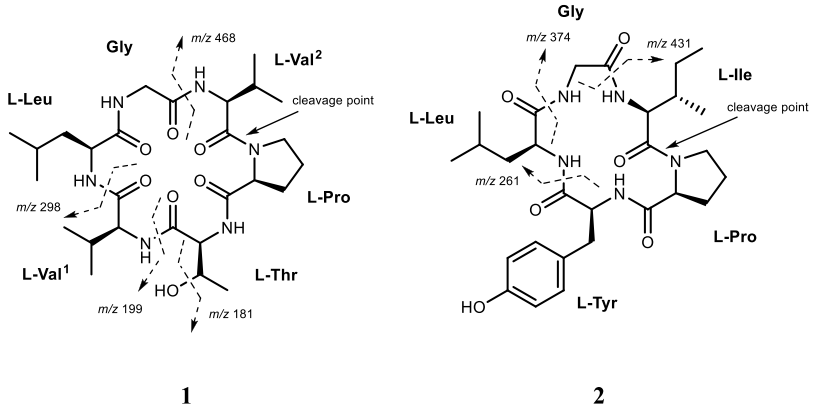

Figure 3. MS/MS fragmentation patterns of compounds **1** and **2**.

HMBC, and COSY analysis proved that **2** consisted of five amino acids, including Pro, Tyr, Leu, Gly, and isoleucine (Ile) (Figure 2). The sequence of constituent amino acid residues was further determined by HMBC analysis. The HMBC correlations from the NH-proton (δ_H 7.09, d, J = 7.2 Hz) of Tyr to the carbonyl carbon (δ_C 170.9) of Pro, from the NH-proton (δ_H 8.66, d, J = 7.4 Hz) of Leu to CO (δ_C 171.1) of Tyr, from the NH-proton (δ_H 7.19, br d, J = 7.6 Hz) of Gly to CO (δ_C 172.2) of Leu, from the NH-proton (δ_H 7.95, d, J = 9.0 Hz) of Ile to CO (δ_C 168.8) of Gly, and from the δ-proton (δ_H 3.40, m) of Pro to CO (δ_C 170.5) of Ile clearly allowed us to determine the sequence to be cyclo (Pro−Tyr−Leu−Gly−Ile). These results were additionally supported by ROESY analysis as well. The absolute configurations of the amino acids constituting **2** were determined by the advanced Marfey's method above, and they all turned out to be of the L-configuration (Table S2 and Figure S46). In the case of Ile, which has one additional stereogenic center at the β position, a different solvent system with trifluoroacetic acid (TFA) was used to refine the obvious differences of retention time (Figure S47). Through the $\Delta\delta_{C\beta-C\gamma}$ values (10.1 ppm) of Pro,[26,27] the amide bond of Ile−Pro was in the *cis* configuration (Table 2). Therefore, the structure of **2** was elucidated as a cyclic pentapeptide with the sequence cyclo (L-Pro−L-Tyr−L-Leu−Gly−L-Ile) and named melicopteline B (**2**).

Melicopteline C (**3**) was isolated as a white and amorphous solid. The molecular formula of **3** was established as $C_{33}H_{41}N_7O_8$ based on a HRESIMS ion peak at m/z 664.3099 $[M + H]^+$, corresponding to 17 degrees of unsaturation. Similar to those of **1** and **2**, one-dimensional (1D) NMR spectrum analysis of **1** indicated the presence of one unit of Val, Thr, and Phe and two units of Gly (Tables 1 and 2). However, some unassigned carbon resonances and the insufficient degree of unsaturation index (five from Phe, one

https://dx.doi.org/10.1021/acs.joc.0c02137
J. Org. Chem. 2021, 86, 1437−1447

Table 2. $^{13}C\{^1H\}$ NMR Data (δ_C in ppm, Type) for Compounds 1−5[a]

position	1		2		3		4		5	
Pro		Pro		HPI		HPI		HPI		
CO	171.03[b], C	CO	170.9, C	CO	171.1, C	CO	172.1, C	CO	171.0, C	
α	60.8, CH	α	61.0, CH	2	62.3, CH	2	62.2, CH	2	62.4, CH	
β	30.8, CH_2	β	31.3, CH	3	41.8, CH2	3	43.5, CH2	3	41.7, CH2	
γ	21.4, CH_2	γ	21.2, CH2	3a	88.0, C	3a	88.4, C	3a	88.1, C	
δ	46.2, CH_2	δ	46.4, CH2	3b	132.1, C	3b	133.0, C	3b	132.0, C	
Thr		Tyr		4	123.0, CH	4	122.8, CH	4	123.0, CH	
CO	172.1, C	CO	171.1, C	5	118.8, CH	5	119.9, CH	5	118.8, CH	
α	58.3, CH	α	54.5, CH	6	129.3, CH	6	129.1, CH	6	129.3, CH	
β	67.3, CH	β	36.8, CH_2	7	110.7, CH	7	111.4, CH	7	110.7, CH	
γ	19.6, CH_3	γ	126.8, C	7a	148.8, C	7a	147.2, C	7a	148.7, C	
Val[1]		*ortho*	130.0, CH	8a	83.6, CH	8a	85.1, CH	8a	83.6, CH	
CO	171.3, C	*meta*	114.8, CH	Val		Val		Val		
α	61.1, CH	*para*	156.0, C	CO	170.6, C	CO	170.0, C	CO	170.8, C	
β	28.5, CH	Leu		α	59.1, CH	α	57.0, CH	α	58.9, CH	
γ	19.0, CH_3	CO	172.2, C	β	30.8, CH	β	30.1, CH	β	31.2, CH	
	18.3, CH_3	α	51.9, CH	γ	18.3, CH3	γ	15.9, CH3	γ	18.1, CH_3	
Leu		β	37.7, CH_2		19.7, CH3		18.5, CH3		19.6, CH_3	
CO	171.02[b], C	γ	24.4, CH	Thr		Thr		Ile		
α	51.4, CH	δ	23.1, CH_3	CO	170.4, C	CO	169.8, C	CO	170.9, C	
β	38.6, CH_2		21.5, CH3	α	56.7, CH	α	56.5, CH	α	56.4, CH	
γ	24.5, CH	Gly		β	66.7, CH	β	65.6, CH	β	38.0, CH	
δ	23.3, CH_3	CO	168.8, C	γ	18.4, CH3	γ	17.1, CH3	γ	19.7, CH2	
	20.7, CH_3	α	42.5, CH_2	Phe		Phe		δ	11.5, CH3	
Gly		Ile		CO	171.0, C	CO	171.6, C	ε	15.3, CH3	
CO	169.5, C	CO	170.5, C	α	56.1, CH	α	56.0, CH	Tyr		
α	42.6, CH_2	α	54.1, CH	β	35.7, CH2	β	38.2, CH2	CO	170.8, C	
Val[2]		β	37.0, CH	γ	138.0, C	γ	136.8, C	α	55.9, CH	
CO	169.4, C	γ	24.1, CH_2	*ortho*	129.0, CH	*ortho*	128.9, CH	β	34.7, CH_2	
α	56.5, CH	δ	11.1, CH_3	*meta*	128.3, CH	*meta*	128.4, CH	γ	127.6, C	
β	29.7, CH	ε	14.6, CH_3	*para*	126.4, CH	*para*	126.6, CH	*ortho*	129.7, CH	
γ	19.1, CH_3			Gly1		Gly1		*meta*	115.0, CH	
	17.8, CH_3			CO	169.1, C	CO	168.8, C	*para*	155.8, C	
				α	42.6, CH_2	α	42.6, CH_2	Gly[1]		
				Gly[2]		Gly[2]		CO	169.4, C	
				CO	168.5, C	CO	167.5, C	α	42.5, CH_2	
				α	42.0, CH_2	α	41.7, CH_2	Gly[2]		
								CO	168.7, C	
								α	41.7, CH_2	

[a]Data were measured in DMSO-d_6 at 200 MHz. [b]These values can be interchangeable.

from Val, one from Thr, and two from two units of Gly out of 17) suggested the presence of another highly conjugated subunit. As shown in Figure 2, extensive analysis of HMBC and $^1H-^1H$ COSY spectra allowed us to find the 3a-hydroxypyrroloindoline (HPI) moiety in the structure,[4] resulting in the satisfaction of the degree of unsaturation index. HMBC correlations from the α-proton (δ_H 4.15, overlap) of Phe to the adjacent CO (δ_C 170.4) of Thr and from the NH-proton (δ_H 7.55, d, J = 6.9 Hz) of Thr to CO (δ_C 170.4) of Thr and CO (δ_C 170.6) of Val demonstrated the connectivity of the subunit (Val−Thr−Phe). In the same manner, HMBC correlations from the α-proton [δ_H 3.94 (dd, J = 16.8, 7.3 Hz) and 3.41 (dd, J = 16.9, 4.8 Hz)] of Gly^1 to CO (δ_C 169.1) of Gly^1 and from the α-proton [δ_H 4.50 (dd, J = 17.0, 8.2 Hz) and 3.89 (d, J = 16.8 Hz)] of Gly^2 to CO (δ_C 168.5) of Gly^2 and CO (δ_C 169.1) of Gly^1 indicated the linkage between two Gly units (Figure S23). Similar to the case of **1**, full sequences of units could be made with the aid of ROESY analysis because of highly overlapped carbon resonances (Figures 2 and S25). The key ROESY correlations between the NH-proton (δ_H 8.66, t, J = 5.5 Hz) of Gly^1 and the α-proton (δ_H 4.15, overlap)/β-proton (δ_H 3.18, dd, J = 14.2, 5.5 Hz) of Phe proved the connectivity of (Val−Thr−Phe−Gly^1−Gly^2). The key ROESY correlations between the α-proton (δ_H 3.89, d, J = 16.8 Hz) of Gly^2 and H-8a (δ_H 5.63, d, J = 3.9 Hz) and between H-2 (δ_H 4.16, overlap)/H-3 (δ_H 2.29, dd, J = 13.4, 5.1 Hz) and the NH-proton (δ_H 7.92, d, J = 12.0 Hz) of Val established the full sequence to be (Val−Thr−Phe−Gly^1−Gly^2−HPI). The absolute configuration in **3** was established using the advanced Marfey's method (Table S2 and Figures S48 and S49). For HPI, ROESY analysis was intensively applied to determine the absolute configurations of the HPI moiety in terms of spatial correlations with the adjacent Val and biosynthetic pathway. The process of determination of the absolute configuration is explained further for compounds **4** and **5** altogether.

Melicopteline C (**4**) was isolated as a white and amorphous solid. The molecular formula of **4** was established as

https://dx.doi.org/10.1021/acs.joc.0c02137
J. Org. Chem. 2021, 86, 1437−1447

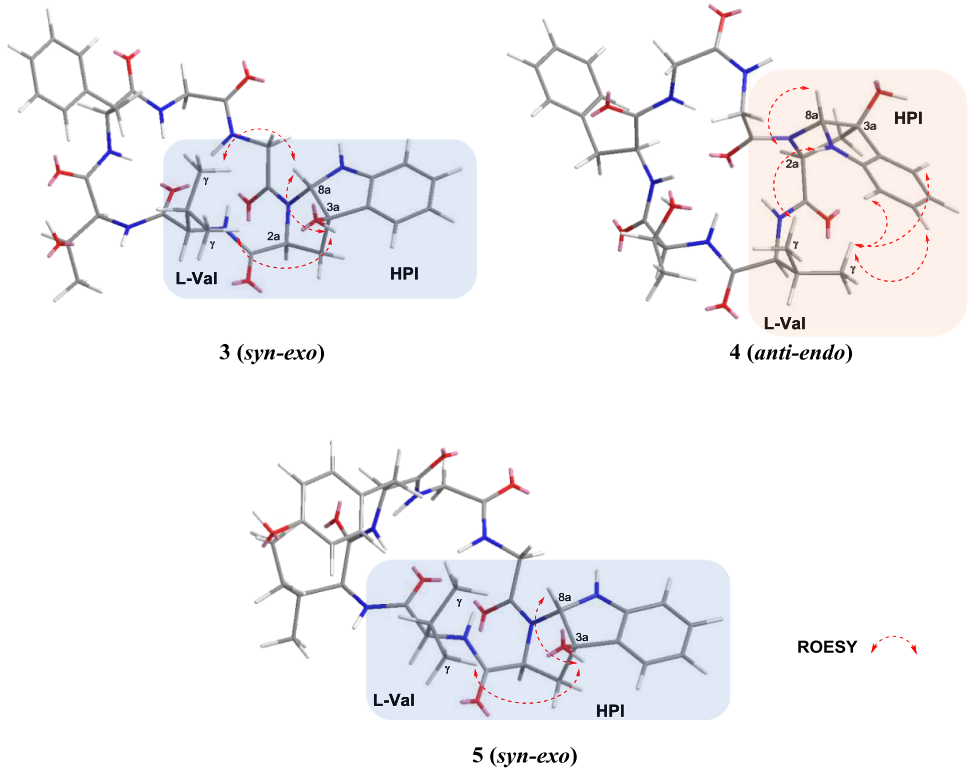

Figure 4. Key correlations of ROESY (dashed arrows) of HPI-containing compounds **3**−**5** for the determination of the absolute configuration of the HPI moiety. The correlations here are mainly focused on the differences of spatial relations between the HPI moiety and the adjacent methyl groups (γ-protons) of Val to determine the absolute configuration of the HPI. It turned out that compounds **3** and **5** adopt a *syn-exo* configuration, whereas compound **4** has a *anti-endo* one.

$C_{33}H_{41}N_7O_8$ based on a HRESIMS ion peak at m/z 664.3123 $[M + H]^+$, corresponding to 17 degrees of unsaturation. The comparison of 1D NMR spectra (Tables 1 and 2) to those of **3** indicated that **4** is an isomer of **3**, also supported by the same molecular weight. When **4** was subjected to advanced Marfey's derivatization, it turned out that all of the amino acids are in L-configurations except for the HPI moiety (Table S2 and Figures S48 and S49). Therefore, it was likely that the difference lay on the absolute configuration of the HPI motif. The absolute configuration of **4** was determined with compounds **3** and **5**.

Melicopteline E (**5**) was isolated as a white and amorphous solid. The molecular formula of **5** was established as $C_{35}H_{45}N_7O_8$ based on a HRESIMS ion peak at m/z 692.3415 $[M + H]^+$, corresponding to 17 degrees of unsaturation. Comparison of 1D NMR spectra to those of **3** demonstrated that **5** also contained one unit of Val and HPI and two units of Gly (Tables 1 and 2). However, ^{1}H NMR peaks [δ_H 6.99 (d, J = 8.0 Hz) and 6.66 (d, J = 8.0 Hz)] integrating for multiples of two in the aromatic region and the indicative triplet methyl group (δ_H 0.74, t, J = 7.2 Hz) with the aid of 2D NMR including ^{1}H−^{1}H COSY indicated that **5** is composed of Tyr and Ile instead of Phe and Thr. The sequence of the constituent amino acid residues was determined by means of HMBC and ROESY analyses (Figure 2). HMBC correlations from the NH-proton (δ_H 7.45, d, J = 1.6 Hz) of Ile to the adjacent CO (δ_C 170.8) of Val and from the NH-proton (δ_H 7.79, d, J = 9.9 Hz) of Val to CO (δ_C 171.0) of HPI and ROESY correlations between the NH-proton of Val and H-2 (δ_H 4.18, overlap)/H-3 (δ_H 2.32, dd, J = 16.7, 4.4 Hz) of HPI suggested the connectivity of the subunit (HPI−Val−Ile). In the same manner, HMBC correlations from the NH-proton (δ_H 8.46, br s) of Gly^1 to CO (δ_C 170.8) of Tyr and from the NH-proton (δ_H 8.14, br d, J = 7.2 Hz) of Gly^2 to CO (δ_C 169.4) of Gly^1 indicated the linkage of (Tyr−Gly^1−Gly^2) (Figures 2 and S39). Owing to the faint correlation spots of HMBC and highly overlapped carbon resonances, the full sequence could be accomplished by the obvious ROESY correlations (Figures 2 and S41). The key ROESY correlations between the NH-proton (δ_H 8.23, s) of Tyr and the α-proton (δ_H 4.28, m)/β-proton (δ_H 1.68, m) of Ile and also between the α-proton (δ_H 3.81, d, J = 15.6 Hz) of Gly^2 and the NH-proton (δ_H 6.90, d, J = 4.5 Hz)/H-8a (δ_H 5.65, d, J = 4.8 Hz) of HPI indicated the full sequence as (Tyr−Gly^1−Gly^2−HPI−Val−Ile). All of the amino acids turned out to be in L-configurations except for the HPI moiety by the advanced Marfey's analysis (Table S2 and Figures S47 and S50).

For the determination of the absolute configurations of HPI, ROESY analysis could be used efficiently as the structure of the cyclopeptide is semirigid, and the configuration of amino acids right next to HPI was determined unambiguously by using a chemical reaction. The pyrroloindole moiety only can be formed in the *cis* junction in either the *exo* or *endo* product when cyclization occurs.[1,13] Also, based on the relationship with regard to the hydroxyl group at C-3a and carboxamido group at C-2, *syn* or *anti* configuration can be deduced, which is determined by whether the HPI is originated from L-Trp or D-Trp.[11,13] Therefore, there are four possibilities (Figure S51) (*syn-exo*, *syn-endo*, *anti-exo*, *anti-endo*). Thus, all four configurations were subjected to the energy minimization with an MM2 forcefield using Chem3D software. L-Val was the

https://dx.doi.org/10.1021/acs.joc.0c02137
J. Org. Chem. 2021, 86, 1437−1447

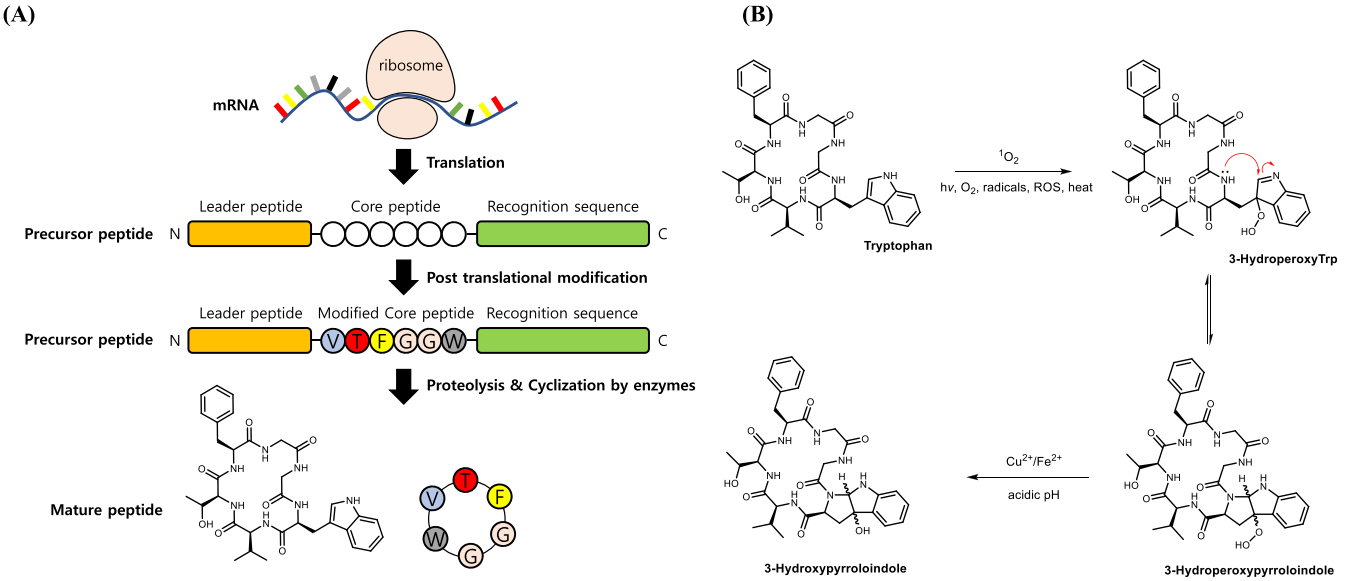

Figure 5. Plausible biosynthetic pathways for compounds **3**−**5**. (**A**) Formation of ribosomally synthesized and post-translationally modified peptides. (**B**) Photooxygenation of tryptophan in compounds **3**−**5**.

key amino acid to determine the chirality of C-2 of HPI. If the H-2 is in the α configuration, the HPI is originated from L-Trp and two methyl groups of the adjacent Val and H-2 of HPI are in anti-cofacial relationship, whereas they are in a cofacial relationship in the case of the β position of H-2 (Figure S52). Extensive analysis of the ROESY data demonstrated that there were no correlations between H-2 and two methyl groups of Val in **3**−**5** (Figures 4 and S53).

Also, the distance between any two methyl groups of Val and either H-8a (OH-3a) or NH of HPI depends on the configuration of H-2. In other words, if H-2 possesses the α configuration, either H-8a (OH-3a) or NH of HPI will be very close to any of the methyl groups of the adjacent Val, regardless of whether the junction is in the *endo* or *exo* configuration (Figure S54). In the β position of H-2, none of the methyl groups are close to H-8a (OH-3a) and NH of HPI (more than 4 Å). In compound **3**, obvious ROESY correlations between H-8a (δ_H 5.63, d, J = 3.9 Hz)/OH-3a (δ_H 6.17, br s) and the methyl group (δ_H 0.86, d, J = 6.8 Hz) of Val were observed (Figures 4 and S55). ROESY correlations between the NH-proton (δ_H 7.20, overlap) of HPI and the methyl group (δ_H 0.50, d, J = 6.9 Hz) of Val and between OH-3a (δ_H 6.29, br s) and the methyl group (δ_H 0.86, d, J = 6.4 Hz) of Val were observed in compounds **4** and **5**, respectively (Figures 4, S33, S41, and S54). Therefore, configurations of the C-2 position in **3**−**5** were adopted as α, which can also be explained by the fact that amino acids of naturally occurring cyclopeptides from plants adopt an L-configuration in most cases. However, the ROESY correlation between H-2 and H-8a was observed in **4**, which means that they are facing the same plane, whereas no correlation was observed in **3** (Figures 4 and S56). Therefore, **3** adopts an *exo* configuration in the junction of HPI, whereas **4** has an *endo* one. These results can also be supported by reported ^{1}H NMR chemical shifts (Table S3 and Figure S57).[13] The previously reported paper clearly showed the differences of chemical shifts of H-2 and H-8a between the synthesized *endo*-configured HPI and the *exo* one. The chemical shifts of H-2 and H-8a in an *exo* form are 3.86 (q, J = 12.0, 7.0 Hz) and 5.40 (s), respectively, whereas, those in the *endo* form are 4.34 (t, J = 7.0 Hz) and 5.31 (s), respectively. The tendency was same with **3** and **4**. The chemical shifts of H-2 and H-8a in **3** are 4.16 (overlap) and 5.63 (d, J = 3.9 Hz), respectively, whereas those in **4** are 4.76 (dd, J = 10.4, 6.0 Hz) and 5.58 (d, J = 4.7 Hz), respectively (Table 1). Interestingly, the pyrrolidine and indoline rings across the junction folded in an *endo* form showed the ROESY correlations between aromatic protons of HPI and methyl groups of Val, whereas no correlation was observed in the *exo* form because of the relatively planar conformation (Figures 4 and S58). In compound **4**, strong ROESY correlations exist between a methyl group (0.50, d, J = 6.9 Hz) and aromatic protons [H-4 (7.21, d, J = 7.5 Hz), H-6 (7.11, t, J = 7.9 Hz), H-7 (6.60, d, J = 7.9)], whereas no correlations were observed in **3**. Therefore, **3** and **4** adopt the *exo* and *endo* form, respectively. With the same logical deduction, the absolute configuration of **5** was also determined to be an *exo* form. There was no ROESY correlation between H-2 (4.18, overlap) and methyl groups of Val (Figure 4), whereas clear correlation between OH-3a (δ_H 6.29, br s) and the methyl group (δ_H 0.86, d, J = 6.4 Hz) was observed, confirming the chirality of H-2 (Figure S41). For the manner of fusion at the ring junction, there were no correlations between H-2 and H-8a (5.65, d, J = 4.8 Hz) and between methyl groups of Val and aromatic protons of HPI. Also, the chemical shifts of H-2 and H-8a are comparable with those of **3** (Table 1).

Biosynthetically, although HPI-bearing molecules, except for cyclopeptides, have been reported, HPI-bearing cylopeptides are very rare in plants. Interestingly, Rutaceae, to which the genus *Melicope* belongs, is one of the major families producing orbitides, which are N-to-C cyclized plant peptides that do not contain a disulfide bond, along with Caryophyllaceae.[28] Orbitides, consisting of smaller cyclic peptides of 5−12 amino acid residues, are initially synthesized by a ribosome to be a precursor peptide in many eukaryotic cells. Then, the core peptide undergoes post-translational modification, followed by proteolysis and cyclization by enzymes in plant cells.[29,30] Tryptophan is also not commonly found in cyclopeptides, is even highly susceptible to oxidation, and is easy to change into other derivatives by stimuli, including UV, heat, or radicals along with methionine, this transformation

https://dx.doi.org/10.1021/acs.joc.0c02137
J. Org. Chem. 2021, 86, 1437−1447

Table 3. Antiviral Activity of Cyclopeptides against Influenza A Viruses H1N1 and H9N2

		EC_{50} (μM)		SI (=CC_{50}/EC_{50})	
compound	CC_{50} (μM)	H1N1	H9N2	H1N1	H9N2
1	>100	5.43 ± 2.32	11.20 ± 2.46	22.53 ± 5.51	9.38 ± 1.61
2	>100	4.75 ± 1.39	9.93 ± 2.94	23.02 ± 4.77	11.04 ± 2.30
3	>100	2.57 ± 0.45	5.47 ± 0.40	40.14 ± 5.60	18.38 ± 1.25
4	>100	3.70 ± 0.25	5.85 ± 1.12	27.15 ± 1.71	17.74 ± 2.75
5	>100	4.28 ± 2.41	6.96 ± 2.28	34.21 ± 8.42	16.10 ± 3.55
Ribavirin[a]	>100	3.92 ± 0.79	2.47 ± 0.98	26.59 ± 4.28	48.05 ± 11.50

[a]Positive control.

being called photooxygenation.[31] In the deprotonated ion peaks in the MS chromatogram, Trp was detected instead of 3a-HPI of compounds **3**–**5** from the EtOAc fraction of the extract of *M. pteleifolia* (Figure S59). Porphyrins, coumarins, and furoquinolines are known to have photosensitive or phototoxic properties.[32,33] Interestingly, *M. pteleifolia* contains a furoquinoline alkaloid as one of its major constituents, and also a variety of furoquinoline alkaloids were detected in a positive mode of mass spectrometry.[32] Therefore, furoquinoline alkaloids in *M. pteleifolia* are highly likely to act as a photosensitizer to aid the photooxygenation reaction of Trp-bearing cyclopeptides. Thus, *M. pteleifolia* may initially produce cyclopeptides that contain Trp rather than intact HPI-bearing ones, and the Trp moiety in cyclopeptides is subjected to photooxygenation by coexisting photosensitizing molecules such as furoquinoline alkaloids to give rise to the HPI moiety (Figure 5).

Influenza A virus has been a continuous threat to human life throughout history by several devastating pandemics such as the "Spanish flu" and "Hong Kong flu". Even though several antivirals, including M2 ion channel blockers of the adamantane class (e.g., amantadine), neuraminidase inhibitors (e.g., oseltamivir and zanamivir), which are most widely prescribed, and recently the polymerase inhibitor baloxavir, have been licensed over the last half a century,[34] many global pharmaceutical companies are making every possible effort to develop anti-influenza virus drugs because of the frequent emergence of drug-resistant viruses. The ethnopharmacological uses of *M. pteleifolia* to relieve various symptoms caused by influenza and the discovery of cyclopeptides containing the rare moiety HPI prompted us to test their anti-influenza activities. As a result, all cyclopeptides showed moderate or strong activity, with an EC_{50} (μM) ranging from 2.57 ± 0.45 to 11.20 ± 2.46 (Table 3). They exhibited stronger activity against the swine influenza subtype, H1N1, than the avian one, H9N2. Interestingly, the HPI moiety-bearing compounds **3**–**5** exerted more potent activity against both subtypes than the normal cyclopeptides **1** and **2**. These results strongly suggest that the HPI motif might increase anti-influenza activity as an important pharmacophore. Among compounds **3**–**5**, compound **3** showed much stronger activity (EC_{50}, 2.57 ± 0.45 μM) than the positive control ribavirin (EC_{50}, 3.92 ± 0.79 μM), with higher selectivity. Considering the fact that initial viral infection can often open doors for secondary bacterial infection,[35] compound **3** can be a promising candidate or lead compound for the development of an anti-influenza agent.

CONCLUSIONS

Five Caryophyllaceae-type cyclopeptides (**1**–**5**) were isolated from the leaves of *M. pteleifolia* by means of acid–base extraction and extensive MS/MS chromatogram analysis. Interestingly, compounds **3**–**5** contains the HPI moiety which is very rare, especially from plants, and their absolute configurations were determined undoubtedly by comprehensive spectroscopic analyses using NMR and MS/MS and advanced Marfey's analysis. Based on the characteristics of the constituents from *M. pteleifolia*, a plausible biosynthetic pathway is suggested. Evaluation of the anti-influenza A virus activity of isolates revealed that all of the cyclopeptides showed antiviral activity; especially, HPI-bearing compounds (**3**–**5**) exhibited more potent activity than the others, suggesting that the HPI motif can exert additive anti-influenza activity and be used as a lead compound for the development of future anti-influenza drugs.

EXPERIMENTAL SECTION

General Experimental Procedures. Optical rotations were recorded on a JASCO P-2000 polarimeter (JASCO International Co. Ltd., Tokyo, Japan). UV and electronic circular dichroism (ECD) spectra were measured using a Chirascan-Plus (Applied Photophysics Ltd., Surrey, UK). IR data were obtained using a Nicolet 6700 Fourier transform infrared spectrometer (Thermo Fisher Scientific, Waltham, MA, USA). 1D and 2D NMR spectra were recorded in deuterated solvents using an AVANCE 800 MHz spectrometer (Bruker, Billerica, MA, USA). HRESIMS was performed using a Waters Xevo G2 QTOF mass spectrometer (Waters MS Technologies, Manchester, UK) equipped with an electrospray ionization (ESI) source. A Gilson HPLC purification system was used for isolation and UV detection at 205 and 254 using an Optima Pak C_{18} column (10 × 250 mm, 5 μm particle size; RS Tech, Seoul, Korea). Regular column chromatography (CC) was carried out with silica gel (particle size: 63–200 μm, Zeochem AG, Rüti, Switzerland), RP-C_{18} (particle size: 75 μm, Nacalai Tesque, Kyoto, Japan), and Sephadex LH-20 (GE Healthcare, Little Chalfont, UK). Silica gel 60 F_{254} and RP-18 F_{254}S TLC plates were obtained from Merck (Darmstadt, Germany). Industrial-grade ethanol, ethyl acetate, and *n*-butanol were used for extraction and purification. Analytical-grade acetonitrile and methanol were used for isolation and analysis. All solvents were purchased from Daejung Chemical (Siheung, Korea). Fluorescence measurements were recorded with a fluorescence microplate reader (Spectra Max Gemini XPS, Molecular Devices, San Jose, CA, USA). Biological data were obtained using a microplate reader (VersaMax, Molecular Devices, San Jose, CA, USA).

Plant Material. The leaves of *M. pteleifolia* were purchased from Ba Vi district, Hanoi, Vietnam, in June 2016. The samples were identified based on morphological characteristics by Dr. Pham of Hanoi University of Pharmacy. A voucher specimen (SNU-12-2016) was deposited in the herbarium of the College of Pharmacy at Seoul National University.

Extraction and Isolation. The leaves of *M. pteleifolia* (5 kg) were extracted with 94.5% EtOH (2 × 13 L, for 2 h each) at 40 °C. The combined extract was concentrated using an evaporator to yield a dry residue (244.8 g). The alkaloid fraction was then prepared using acid–base extraction as follows. The crude extract was suspended in

https://dx.doi.org/10.1021/acs.joc.0c02137
J. Org. Chem. 2021, 86, 1437–1447

5% HCl aqueous solution and then partitioned with EtOAc three times. The water layer was basified with KOH and successively partitioned with EtOAc three times, resulting in 3.2 g of the alkaloid fraction. The alkaloid fraction (3.2 g) was subjected to Sephadex LH-20 open CC with an isocratic solvent system of 100% MeOH to obtain 10 subfractions (F.1−F.10). F.5 (32 mg) was subjected to semipreparative HPLC with CH_3CN/H_2O (v/v, 40/60) containing 0.05% formic acid (flow rate, 4 mL/min), resulting in the isolation of compound **1** (5.3 mg, t_R = 7.7 min). F.7 (25 mg) was subjected to semipreparative HPLC with CH_3CN/H_2O (v/v, 40/60) containing 0.05% formic acid (flow rate, 4 mL/min), resulting in the isolation of compound **2** (3.4 mg, t_R = 10.8 min). F.9 (1.4 g) was subjected to medium pressure liquid chromatography with a gradient solvent system of MeOH/H_2O (v/v, 10/90 → 100/0) containing 0.05% formic acid to obtain subfractions (F.9.1−F.9.20). F.9.12 (130 mg) was applied to Sephadex LH-20 open CC with an isocratic solvent system of 100% MeOH to obtain nine subfractions (F.9.12.1−F.9.12.9). F.9.12.9 (44.2 mg) was applied to semipreparative HPLC with CH_3CN/H_2O (v/v, 29/71) containing 0.05% formic acid (flow rate, 2 mL/min) to obtain compound **3** (4.2 mg, t_R = 23.8 min), compound **4** (2.4 mg, t_R = 26.9 min), and compound **5** (3.5 mg, t_R = 31.5 min).

*Melicopteline A (**1**).* Yellow amorphous solid; $[\alpha]_D^{20}$ −39.5 (*c* 0.4, MeOH); UV (MeOH) λ_{max} (log ε) 200 (4.0), 269 (2.7) nm; CD (MeOH) ($\Delta\varepsilon$) 221 (−4.0); IR ν_{max}: 3311, 2967, 1638, 1545, 1454, 1055 cm^{-1}; ^1H and $^{13}C\{^1H\}$ NMR data, see Tables 1 and 2; HRMS (ESI) *m*/*z*: $[M + H]^+$ calcd for $C_{27}H_{47}N_6O_7$, 567.3506, found, 567.3517.

*Melicopteline B (**2**).* Pale yellow amorphous solid; $[\alpha]_D^{20}$ −24.7 (*c* 0.4, MeOH); UV (MeOH) λ_{max} (log ε) 200 (4.3), 225 (3.9), 275 (3.4) nm; CD (MeOH) ($\Delta\varepsilon$) 222 (−3.7); IR ν_{max}: 3303, 2966, 1655, 1517, 1455, 1369 cm^{-1}; ^1H and $^{13}C\{^1H\}$ NMR data, see Tables 1 and 2; HRMS (ESI) *m*/*z*: $[M + H]^+$ calcd for $C_{28}H_{42}N_5O_6$, 544.3135, found, 544.3134.

*Melicopteline C (**3**).* White amorphous solid; $[\alpha]_D^{20}$ +2.6 (*c* 0.37, MeOH); UV (MeOH) λ_{max} (log ε) 201 (4.0), 235 (3.1), 289 (2.7) nm; CD (MeOH) ($\Delta\varepsilon$) 214 (−1.1), 227 (−1.1); IR ν_{max}: 3435, 2969, 1734, 1653, 1560, 1033 cm^{-1}; ^1H and $^{13}C\{^1H\}$ NMR data, see Tables 1 and 2; HRMS (ESI) *m*/*z*: $[M + H]^+$ calcd for $C_{33}H_{42}N_7O_8$, 664.3095, found 664.3099.

*Melicopteline D (**4**).* White amorphous solid; $[\alpha]_D^{20}$ +30.8 (*c* 0.4, MeOH); UV (MeOH) λ_{max} (log ε) 201 (4.1), 233 (3.3), 288 (2.8) nm; CD (MeOH) ($\Delta\varepsilon$) 212 (−0.9), 231 (−1.7); IR ν_{max}: 3317, 2966, 1654, 1560, 1032 cm^{-1}; ^1H and $^{13}C\{^1H\}$ NMR data, see Tables 1 and 2; HRMS (ESI) *m*/*z*: $[M + H]^+$ calcd for $C_{33}H_{42}N_7O_8$, 664.3095, found, 664.3123.

*Melicopteline E (**5**).* White amorphous solid; $[\alpha]_D^{20}$ −10.5 (*c* 0.4, MeOH); UV (MeOH) λ_{max} (log ε) 201 (4.7), 226 (4.1), 284 (3.6) nm; CD (MeOH) ($\Delta\varepsilon$) 226 (4.1), 284 (3.6); IR $\nu_{max:}$ 3318, 2966, 1644, 1518, 1438, 1282, 1033 cm^{-1}; ^1H and $^{13}C\{^1H\}$ NMR data, see Tables 1 and 2; HRMS (ESI) *m*/*z*: $[M + H]^+$ calcd for $C_{35}H_{46}N_7O_8$, 692.3408, found, 692.3415.

Advanced Marfey's Analysis for Compounds 1−5.[25,36,37] Compounds **1**−**5** (0.5 mg each) were hydrolyzed with 6 *N* HCl (200 μL) at 115 °C for 1.5 h. The residual HCl was removed using a rotary evaporator. The dried hydrolysates of **1**−**5** were suspended in H_2O (20 μL) and treated with 1 M $NaHCO_3$ (20 μL) and 25 mM L-FDLA in acetone (100 μL). The solutions were heated at 37 °C for 1 h. The reaction was quenched by adding 20 μL of 1 *N* HCl and diluted with CH_3CN. Aliquots of the solutions were used for the subsequent HPLC analysis. For comparison with the derivatives of authentic standard amino acids, pairs of L- and D-Val, Tyr, Leu, Pro, Thr, allo-Thr, Ile, allo-Ile, and Phe were also derivatized successfully with L-FDLA. The retention times of amino acids derivatives in **1**−**5** were compared with those of authentic ones. Especially, Thr was analyzed by HPLC−ESI-MS for clarity, and a 5 μm Kinetex C-18 column (250 × 4.6 mm, 100 Å) was eluted at 0.4 mL min^{-1} [0.1% HCOOH in H_2O and CH_3CN] with the gradient system (20 → 80% CH_3CN over 15 min, isocratic 80% CH_3CN over 5 min). The retention time (t_R = 17.09) with mass (412 *m*/*z* from extraction ion chromatogram of the negative mode) of the derivative of Thr in **1** was compared with that of L-Thr (t_R = 17.08), D-Thr (t_R = 18.53), L-all-Thr (t_R = 17.41), and D-all-Thr (t_R = 17.96), assigning its absolute configuration to be L-Thr. In the same manner, Thr in **3** and **4** was determined to be L-Thr (Figures S45 and S49). For Ile, the gradient system (25 → 60% CH_3CN over 70 min) at 1.0 mL min^{-1} [0.05% TFA in H_2O and CH_3CN] was used. The retention time (t_R = 37.27) of Ile in **2** was compared with that of L-Ile (t_R = 37.29), L-all-Ile (t_R = 36.86), D-Ile (t_R = 50.19), and D-all-Ile (t_R = 50.19), assigning its absolute configuration to be L-Ile (Figure S47). In the same manner, Ile in **5** was also determined to be L-Ile. For the rest of the amino acids, the gradient system (20 → 65% CH_3CN over 35 min) at 1.0 mL min^{-1} [H_2O and 0.1% HCOOH in CH_3CN] was used. The retention times of the derivatives of amino acids in **1**−**5** were compared to those of authentic ones and determined to be L-form (Table S2 and Figures S44, S46 and S48).

Cytopathic Effect Inhibition Assay.[38,39] MDCK cells were seeded on 96-well culture plates at a density of 1×10^5 cells per well. After incubation for 24 h, the medium was removed, and the cells were washed twice with phosphate-buffered saline (PBS). The influenza H1N1 and H9N2 viruses at a multiplicity of infection of 0.01 were inoculated onto near-confluent MDCK cell monolayers using Dulbecco's modified Eagle's medium (DMEM) containing 0.15 μg/mL trypsin and 5 μg/mL bovine serum albumin for 2 h. The medium was removed, the cells were washed with PBS, and new medium with several compounds at different concentrations was added. After being incubated for 3 days at 37 °C under a 5% CO_2 atmosphere, the cell medium was replaced with DMEM, 20 μL of 2 mg/mL MTT was added to each well, and the plate was incubated for 4 h at 37 °C. After that, the subsequent steps followed those of the cytotoxicity assay procedures, and the 50% effective concentration (EC_{50}) was evaluated by regression analysis. A selective index (SI) value was determined via the formula SI = CC_{50}/EC_{50}. The statistical significance was calculated via comparison with the null group.

■ ASSOCIATED CONTENT

Supporting Information

The Supporting Information is available free of charge at https://pubs.acs.org/doi/10.1021/acs.joc.0c02137.

1D and 2D NMR, HRESIMS, ECD spectra, and chromatograms after advanced Marfey's analysis of compounds **1**−**5**; comparison of retention times of derivatized amino acids in **1**−**5** to those of authentic amino acids; and processes of logical deduction to determine the absolute configuration of the HPI moiety using extensive ROESY analysis (PDF)

■ AUTHOR INFORMATION

Corresponding Author

Won Keun Oh − *Korea Bioactive Natural Material Bank, Research Institute of Pharmaceutical Sciences, College of Pharmacy, Seoul National University, Seoul 08826, Republic of Korea;* orcid.org/0000-0003-0761-3064; Phone: +82-2-880-7872; Email: wkoh1@snu.ac.kr

Authors

Ba Wool Lee − *Korea Bioactive Natural Material Bank, Research Institute of Pharmaceutical Sciences, College of Pharmacy, Seoul National University, Seoul 08826, Republic of Korea;* orcid.org/0000-0002-4944-5145

Thi Kim Quy Ha − *Korea Bioactive Natural Material Bank, Research Institute of Pharmaceutical Sciences, College of Pharmacy, Seoul National University, Seoul 08826, Republic of Korea; Cantho University, Cantho City 900000, Vietnam*

Eun Jin Park − *Korea Bioactive Natural Material Bank, Research Institute of Pharmaceutical Sciences, College of*

https://dx.doi.org/10.1021/acs.joc.0c02137
J. Org. Chem. 2021, 86, 1437−1447

Pharmacy, Seoul National University, Seoul 08826, Republic of Korea

Hyo Moon Cho − *Korea Bioactive Natural Material Bank, Research Institute of Pharmaceutical Sciences, College of Pharmacy, Seoul National University, Seoul 08826, Republic of Korea;* orcid.org/0000-0003-3447-8726

Byeol Ryu − *Korea Bioactive Natural Material Bank, Research Institute of Pharmaceutical Sciences, College of Pharmacy, Seoul National University, Seoul 08826, Republic of Korea;* orcid.org/0000-0002-3405-2875

Thi Phuong Doan − *Korea Bioactive Natural Material Bank, Research Institute of Pharmaceutical Sciences, College of Pharmacy, Seoul National University, Seoul 08826, Republic of Korea*

Hee Ju Lee − *Korea Bioactive Natural Material Bank, Research Institute of Pharmaceutical Sciences, College of Pharmacy, Seoul National University, Seoul 08826, Republic of Korea; Natural Product Informatics Research Center, Korea Institute of Science and Technology, Gangneung 25451, Republic of Korea*

Complete contact information is available at: https://pubs.acs.org/10.1021/acs.joc.0c02137

Notes

The authors declare no competing financial interest.

■ ACKNOWLEDGMENTS

This work was supported financially by grants from the Korea Bioactive Natural Material Bank (NRF-2017M3A9B8069409) of the National Research Foundation of Korea (NRF) which is funded by the Ministry of Science and ICT, and the Korea Institute of Planning and Evaluation for Technology in Food, Agriculture and Forestry (IPET) through the Animal Disease Management Technology Development Program funded by the Ministry of Agriculture, Food and Rural Affairs (MAFRA) (318031031SB010).

■ REFERENCES

(1) Ruiz-Sanchis, P.; Savina, S. A.; Albericio, F.; Álvarez, M. Structure, bioactivity and synthesis of natural products with hexahydropyrrolo[2,3-b]indole. *Chem.—Eur. J.* **2011**, *17*, 1388−1408.

(2) Ishikura, M.; Abe, T.; Choshi, T.; Hibino, S. Simple indole alkaloids and those with a non-rearranged monoterpenoid unit. *Nat. Prod. Rep.* **2013**, *30*, 694−752.

(3) Witkop, B. From the "ordeal bean" (*Physostigma venenosum*) to the ordeal of Alzheimer's disease - some of the legacy of Percy Lavon Julian. *Heterocycles* **1998**, *49*, 9−27.

(4) Bunders, C.; Cavanagh, J.; Melander, C. Flustramine inspired synthesis and biological evaluation of pyrroloindoline triazole amides as novel inhibitors of bacterial biofilms. *Org. Biomol. Chem.* **2011**, *9*, 5476−5481.

(5) He, B.; Song, H.; Du, Y.; Qin, Y. Total synthesis of (−)-ardeemin. *J. Org. Chem.* **2009**, *74*, 298−304.

(6) Takase, S.; Kawai, Y.; Uchida, I.; Tanaka, H.; Aoki, H. Structure of amauromine, a new alkaloid with vasodilating activity produced by *Amauroascus* sp. *Tetrahedron Lett.* **1984**, *25*, 4673−4676.

(7) Dolby, L. J.; Nelson, S. J. Model studies of the synthesis of echitamine and related indole alkaloids. *J. Org. Chem.* **1973**, *38*, 2882−2887.

(8) Büchel, E.; Martini, U.; Mayer, A.; Anke, H.; Sterner, O. Omphalotins B, C and D, nematicidal cyclopeptides from *Omphalotus olearius*. Absolute configuration of omphalotin A. *Tetrahedron* **1998**, *54*, 5345−5352.

(9) Pettit, G. R.; Tan, R.; Herald, D. L.; Williams, M. D.; Cerny, R. L. Antineoplastic agents. 277. Isolation and structure of phakellistatin 3 and isophakellistatin 3 from a Republic of comoros marine sponge. *J. Org. Chem.* **1994**, *59*, 1593−1595.

(10) Fujimori, D. G.; Hrvatin, S.; Neumann, C. S.; Strieker, M.; Marahiel, M. A.; Walsh, C. T. Cloning and characterization of the biosynthetic gene cluster for kutznerides. *Proc. Natl. Acad. Sci. U.S.A.* **2007**, *104*, 16498−16503.

(11) Kamenecka, T. M.; Danishefsky, S. J. Studies in the total synthesis of himastatin: a revision of the stereochemical assignment. *Angew. Chem., Int. Ed.* **1998**, *37*, 2993−2995.

(12) Umezawa, K.; Ikeda, Y.; Uchihata, Y.; Naganawa, H.; Kondo, S. Chloptosin, an apoptosis-inducing dimeric cyclohexapeptide produced by Streptomyces. *J. Org. Chem.* **2000**, *65*, 459−463.

(13) Nakagawa, M.; Kato, S.; Kataoka, S.; Kodato, S.; Watanabe, H.; Okajima, H.; Hino, T.; Witkop, B. Dye-sensitized photooxygenation of tryptophan: 3a-hydroperoxypyrroloindole as a labile precursor of formylkynurenine. *Chem. Pharm. Bull.* **1981**, *29*, 1013−1026.

(14) Zhang, Y.; Yang, L.-J.; Jiang, K.; Tan, C.-H.; Tan, J.-J.; Yang, P.-M.; Zhu, D.-Y. Glycosidic constituents from the roots and rhizomes of *Melicope pteleifolia*. *Carbohydr. Res.* **2012**, *361*, 114−119.

(15) Nguyen, N. H.; Ha, T. K. Q.; Choi, S.; Eum, S.; Lee, C. H.; Bach, T. T.; Chinh, V. T.; Oh, W. K. Chemical constituents from *Melicope pteleifolia* leaves. *Phytochemistry* **2016**, *130*, 291−300.

(16) Yao, Q.; Gao, Y.; Lai, C.; Wu, C.; Zhao, C.-L.; Wu, J.-L.; Tang, D.-X. The phytochemistry, pharmacology and applications of *Melicope pteleifolia*: a review. *J. Ethnopharmacol.* **2020**, *251*, 112546.

(17) Chen, F. K.; Lu, L. N.; Sun, Z. M. Clinical efficacy of Sanjiuweitai particles in the treatment of chronic gastritis. *Chin. J. Clin. Ration. Drug Use* **2012**, *5*, 69−70.

(18) Lv, L. Y.; Zhou, L. Q. Therapeutic observation of *Evodia lepta* prescription in 118 cases of patients with upper respiratory tract infections. *Mediators Inflammation* **2007**, *20*, 827−828.

(19) Pan, Y.; Huang, X. F.; Li, Y. S. Clinical observation of compound Ganmaoling granules in 60 cases of cold patients. *Yunnan. J. Tradit. Chin. Med. Mat. Med.* **2007**, *28*, 31−32.

(20) Kim, H. J.; Choi, J. H.; Hwang, J. H.; Kim, K. S.; Noh, J. R.; Choi, D. H.; Moon, S. J.; Kim, H. Y.; Kim, S. W.; Choi, S.; Eum, S. M.; Bach, T. T.; Rho, J.; Lee, J. Y.; Park, J. G.; Oh, S. R.; Lee, C. H.; Oh, W. K.; Kim, Y. H. 3,5-Di-C-β-D-glucopyranosyl phloroacetophenone, a major component of *Melicope ptelefolia*, suppresses fibroblast activation and alleviates arthritis in a mouse model: Potential therapeutics for rheumatoid arthritis. *Int. J. Mol. Med.* **2018**, *42*, 2763−2775.

(21) Mahadi, M.; Abdul Rahman, N.; Viswanathan, D.; Taib, I. S.; Sulong, A.; Hakeem, W. A.; Mohamad, M.; Khalid Mohammed, I.; Abidin, I. I. Z.; Rahman, S. A.; Yusuf, Z. The potential effects of *Melicope ptelefolia* root extract as an anti-nociceptive and anti-inflammatory on animal models. *Bull. Fac. Pharm. Cairo Univ.* **2016**, *54*, 237−241.

(22) Kabir, M. F.; Mohd, A. J.; Abolmaesoomi, M.; Hashim, O. H. *Melicope ptelefolia* leaf extract exhibit antioxidant activity and exert antiproliferative effect with apoptosis induction on four different cancer cell lines. *BMC Complementary Altern. Med.* **2017**, *17*, 252.

(23) Lee, B.-W.; Park, J.-G.; Ha, T. K. Q.; Pham, H. T. T.; An, J.-P.; Noh, J.-R.; Lee, C.-H.; Oh, W.-K. Constituents of the edible leaves of *Melicope pteleifolia* with potential analgesic activity. *J. Nat. Prod.* **2019**, *82*, 2201−2210.

(24) Breci, L. A.; Tabb, D. L.; Yates, J. R., III; Wysocki, V. H. Cleavage N-terminal to proline: analysis of a database of peptide tandem mass spectra. *Anal. Chem.* **2003**, *75*, 1963−1971.

(25) Fujii, K.; Ikai, Y.; Oka, H.; Suzuki, M.; Harada, K.-i. A nonempirical method using LC/MS for determination of the absolute configuration of constituent amino acids in a peptide: combination of Marfey's method with mass spectrometry and its practical application. *Anal. Chem.* **1997**, *69*, 5146−5151.

(26) Afifi, A. H.; El-Desoky, A. H.; Kato, H.; Mangindaan, R. E. P.; de Voogd, N. J.; Ammar, N. M.; Hifnawy, M. S.; Tsukamoto, S. Carteritins A and B, cyclic heptapeptides from the marine sponge *Stylissa carteri*. *Tetrahedron Lett.* **2016**, *57*, 1285−1288.

(27) Siemion, I. Z.; Wieland, T.; Pook, K.-H. Influence of the distance of the proline carbonyl from the β and γ carbon on the ^{13}C chemical shifts. *Angew. Chem., Int. Ed.* **1975**, *14*, 702−703.
(28) Luo, S.; Dong, S.-H. Recent advances in the discovery and biosynthetic study of eukaryotic RiPP natural products. *Molecules* **2019**, *24*, 1541.
(29) Ortega, M. A.; van der Donk, W. A. New insights into the biosynthetic logic of ribosomally synthesized and post-translationally modified peptide natural products. *Cell Chem. Biol.* **2016**, *23*, 31−44.
(30) Fisher, M. F.; Payne, C. D.; Chetty, T.; Crayn, D.; Berkowitz, O.; Whelan, J.; Rosengren, K. J.; Mylne, J. S. The genetic origin of evolidine, the first cyclopeptide discovered in plants, and related orbitides. *J. Biol. Chem.* **2020**, *295*, 14510−14521.
(31) Bellmaine, S.; Schnellbaecher, A.; Zimmer, A. Reactivity and degradation products of tryptophan in solution and proteins. *Free Radical Biol. Med.* **2020**, *160*, 696−718.
(32) Towers, G.; Graham, E.; Spenser, I.; Abramowski, Z. Phototoxic furanoquinolines of the Rutaceae. *J. Med. Plants Res.* **1981**, *41*, 136−142.
(33) Schimmer, O.; Kühne, I. Furoquinoline alkaloids as photosensitizers in *Chlamydomonas reinhardtii*. *Mutat. Res.* **1991**, *249*, 105−110.
(34) Hurt, A. C. Antiviral therapy for the next influenza pandemic. *Trop. Med. Infect. Dis.* **2019**, *4*, 67.
(35) Skalickova, S.; Heger, Z.; Krejcova, L.; Pekarik, V.; Bastl, K.; Janda, J.; Kostolansky, F.; Vareckova, E.; Zitka, O.; Adam, V.; Kizek, R. Perspective of use of antiviral peptides against influenza virus. *Viruses* **2015**, *7*, 5428−5442.
(36) Hashizume, H.; Iijima, K.; Yamashita, K.; Kimura, T.; Wada, S.-i.; Sawa, R.; Igarashi, M. Valgamicin C, a novel cyclic depsipeptide containing the unusual amino acid cleonine, and related valgamicins A, T and V produced by *Amycolatopsis* sp. ML1-hF4. *J. Antibiot.* **2018**, *71*, 129−134.
(37) Kaweenwan, I.; Komaki, H.; Hemmi, H.; Hoshino, K.; Hosaka, T.; Isokawa, G.; Oyoshi, T.; Kodani, S. Isolation and structure determination of a new cytotoxic peptide, curacozole, from *Streptomyces curacoi* based on genome mining. *J. Antibiot.* **2019**, *72*, 1−7.
(38) Barrio, G. d.; Spengler, I.; García, T.; Roque, A.; Álvarez, Á. L.; Calderón, J. S.; Parra, F. Antiviral activity of *Ageratina havanensis* and major chemical compounds from the most active fraction. *Braz. J. Pharm. Sci.* **2011**, *21*, 915−920.
(39) Cho, H. M.; Doan, T. P.; Ha, T. K. Q.; Kim, H. M.; Lee, B. W.; Pham, H. T. T.; Cho, T. O.; Oh, W. K. Dereplication by high-performance liquid chromatography (HPLC) with quadrupole-time-of-flight mass spectroscopy (qTOF-MS) and antiviral activities of phlorotannins from *Ecklonia cava*. *Mar. Drugs* **2019**, *17*, 149.

https://dx.doi.org/10.1021/acs.joc.0c02137
J. Org. Chem. 2021, 86, 1437−1447